Journal of Crystal Growth 377 (2013) 9–16

Contents lists available at SciVerse ScienceDirect

Journal of Crystal Growth

journal homepage: www.elsevier.com/locate/jcrysgro

Crystal shape 2D modeling for transient CZ silicon crystal growth

A. Sabanskis [a,*], K. Bergfelds [a], A. Muiznieks [a,†], Th. Schröck [b], A. Krauze [a]

[a] Faculty of Physics and Mathematics, University of Latvia, Zeļļu Street 8, LV-1002, Riga, Latvia
[b] Siltronic AG, Hanns-Seidel-Platz 4, D-81737 München, Germany

ARTICLE INFO

Article history:
Received 11 February 2013
Received in revised form
27 April 2013
Accepted 29 April 2013
Communicated by Chung wen Lan
Available online 7 May 2013

Keywords:
A1. Computer simulation
A1. Phase boundaries
A1. Heat transfer
A2. Czochralski method
A2. Growth from melt

ABSTRACT

A non-stationary axisymmetric model of Czochralski silicon single crystal growth is presented. The model describes transient behavior of crystal–melt, melt–gas and crystal–gas interfaces in connection with PID-based control of crystal diameter by changing crystal pulling velocity and heater power. To calculate significant crystal shape changes, unstructured finite element mesh is used in crystal and melt together with automatic element size control. Heater temperature changes are modeled with a simplified integral model. A numerical simulation example of start cone growth is given.

1. Introduction

Nowadays, the Czochralski (CZ) process is widely used for the production of large single crystals with desired properties. For example, monocrystalline ingots of such semiconductors as silicon or gallium arsenide are typically grown by the CZ method. The mathematical model of CZ process is complex because the complete crystal growth process, which starts with dipping the small-sized seed crystal into the melt and slowly pulling the growing crystal of desired shape upwards, is in its nature transient. Moreover, multiple physical phenomena have to be taken into account, which is still a very challenging task [1].

One of the first realistic calculations of significantly changing crystal diameter, i.e., "shouldering" (cone growth), during global simulation of transient CZ process is presented in Refs. [2,3]. The axisymmetric mathematical model describes the non-stationary temperature field and radiation heat exchange as well as time-dependent crystal–melt, melt–gas and crystal–gas interface shapes. Direct and inverse problems are considered; in the former, the system time evolution is calculated using the provided heater power curve; in the latter, the required heater power curve necessary to obtain the imposed crystal shape is calculated. Nevertheless, a constant structural mesh topology is used in calculations and process control is not considered for the solving of the inverse problem.

The dynamic modeling of oxide crystal CZ growth with the PID-type process control is considered in Refs. [4,5]. Because of the high Prandtl number for oxide melts, the convective heat transfer is taken into account in the melt. In these calculations the change of crystal radius is considered and the weight-based control is used to obtain a desired crystal shape. Nevertheless, structural grids are used in the crystal and melt, making this approach technically limited for precise calculation of crystal diameter changes.

An example of a low-order modeling approach is given in Ref. [6], where the shape of the crystallization interface is represented by a several piecewise linear segments. The whole system is divided in a number of lumps and for each lump heat flow balance is related with the corresponding temperature change rates. This approach describes system dynamics and is computationally inexpensive, therefore it can be used to support an experiment in real-time. Feedback from an experiment can be used to increase numerical model precision. However, this model could not be considered as a self-contained model with high enough precision.

Because of the importance of process control for CZ growth, it is a topic of active research. State-of-the-art works [7–10] deal with, among other things, the reconstruction of parameters that cannot be directly measured by a nonlinear state observer and optimal design of CZ control system. Of course, these references are by no means complete—a good survey of the works considering model-based approach for CZ control as well as control design is given in Ref. [11, chap. 3], see also references therein. Since we are

* Corresponding author. Tel.: +371 67033796; fax: +371 67033751.
E-mail address: andrejs.sabanskis@lu.lv (A. Sabanskis).
† Deceased.

0022-0248/$ - see front matter © 2013 Elsevier B.V. All rights reserved.
http://dx.doi.org/10.1016/j.jcrysgro.2013.04.055

currently focusing on the development of the mathematical model for transient CZ growth simulation, we feel that at this stage process control details are not of great significance. Nevertheless, the exact control design and its parameters are important and our model could be readily used for precise tests of different control approaches.

Possibility of 3D calculations of the three-phase boundary movement in horizontal and vertical directions for CZ process is shown in Refs. [12,13]. The influence of melt motion on heat transfer in the melt is taken into account. Nevertheless, structural grid is used and only small changes of crystal shape are considered. 3D calculations of crystal shape, including facets, are reported in Ref. [14]. However, this model includes growth kinetics and due to 3D description demands high computer resources, therefore it is unsuitable for efficient calculations of transient silicon crystal growth processes with control.

Examples of commercial codes for modeling CZ crystal growth are CGSim package [1,4,5,15,16] and FEMAG-CZ simulation software [17,18]. It is possible to calculate the non-stationary temperature fields, crystallization interface and crystal diameter changes, and to solve direct and inverse problems. However, even if unstructured meshes can be used, as demonstrated in Ref. [18] for a 100 mm CZ silicon growth, the underlying mathematical model for dealing with moving unstructured meshes as well as an example of a full process control for an industrial-scale (200 or 300 mm in diameter) silicon crystal growth are still not published.

To sum up, there is a necessity for an effective mathematical model of transient CZ process that can accurately describe changes of phase boundaries, especially in the vicinity of the triple point (TP), and can distinguish very small crystal shape changes and therefore could be used to consider CZ process with crystal diameter control by changing crystal pulling velocity and heater power.

In the present paper we propose a mathematical model which is (i) axisymmetric and with simplified heater description, therefore computationally inexpensive yet realistic; (ii) fully transient (non-stationary); (iii) with focus on the triple point region and crystal shape formation, for which an unstructured mesh is used. Our model is based on previously developed transient model for floating zone crystal growth process [19,20] and is implemented in program CZ-Trans. An example of crystal shape calculations for CZ silicon single crystal start cone growth is given and the processes in the vicinity of TP are analyzed.

2. Mathematical model and calculation algorithm

A simplified CZ system is schematically shown in Fig. 1. It consists of crystal and melt domains in which non-stationary axisymmetric temperature field is calculated. Melt temperature is kept above the melting point using a graphite heater. Due to the relatively good graphite heat conductivity, for the heater a simplified description is used with an uniform but time-dependent effective temperature. Optionally, the influence of an additional radiating surface (e.g., heat shield) can be taken into account.

The proposed mathematical model describes heat transfer in crystal and melt by heat conduction. Optionally, the heat conduction in the crucible wall can be taken into account. The influence of convective heat transfer by melt flow is neglected in the present model (or modeled with enhanced heat conductivity). The thermal radiation is described by view factors. It is assumed that the horizontal part of the melt free surface does not change its vertical position due to ideally controlled crucible movement. The meniscus shape at the TP is modeled in hydrostatic approximation. The shape of the crystallization interface and the changes of crystal length and crystal radius are also modeled. For faster calculations,

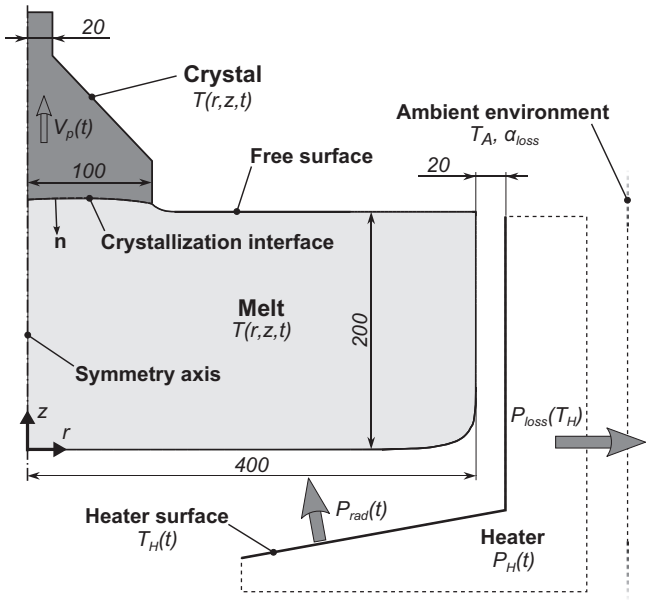

Fig. 1. A simplified CZ system (dimensions in millimeters).

the assumption of constant melt volume is used while considering systems with large melt volumes and time intervals in which there are relatively small crystal volume increases.

The general calculation algorithm as implemented in program CZ-Trans is the following:

1. In the beginning of a new time step, crystal pulling velocity and heater power are adjusted accordingly to the desired crystal side surface shape and to desired pulling velocity. For this the conventional PID-based control is used, see Section 2.1. A simplified heater model, which connects the changes of heater power and temperature is given in Section 2.2.
2. The previously calculated crystal growth velocities along the crystallization interface, the previous crystallization interface and previous meniscus shape at TP are used to calculate the new shape of crystallization interface and the new position of TP. Then the whole crystal (i.e., previous FEM mesh) is moved upwards accordingly to current crystal pulling velocity and time step, see Section 2.3.
3. Using the new TP position above the melt level, free surface shape (meniscus) is calculated, see Section 2.4.
4. New mesh which is appropriate to the new geometry is generated in crystal and melt; temperature field is interpolated from old mesh to the new one.
5. Coupled temperature-radiation problem is solved iteratively for the next time instant, see Section 2.5.
6. From obtained temperature fields, the heat flux density distributions along crystallization interface and corresponding crystal growth velocities are calculated.

Detailed explanation of the most important calculation steps is given below.

2.1. Process PID control

In order to grow a crystal of the desired side surface shape with desired pulling velocity, two PID controllers are used as follows [11, sect. 3.5]:

1. a crystal diameter PID controller (denoted by index "*D*"), in which the difference between actual and desired crystal

diameter value is used as signal for the enhancement of pulling velocity, V_p, relative to the reference value;
2. a heater power PID controller (denoted by index "H"), in which the difference between actual and desired pulling velocity is used as signal for the enhancement of heater power, P_H, relative to the given reference value.

Crystal pulling velocity changes control crystal diameter much faster than heater temperature due to thermal inertia of system components.

The standard form of the PID controller is used, in which the change Δu of the manipulated variable u is given by

$$\Delta u(t) = K_p\left(e(t) + T_d\frac{de}{dt}(t) + \frac{1}{T_i}\int_0^t e(\tau)\,d\tau\right), \tag{1}$$

where $e(t) = f_0(t) - f(t)$ is the difference between setpoint (target value) f_0 and actual value of process variable f, K_p is the gain, T_i and T_d are the integral time and the derivative time, correspondingly. The manipulated variable is adjusted accordingly to $u(t) = u^{\mathrm{ref}}(t) + \Delta u(t)$, with an externally provided reference curve u^{ref}.

2.2. Simplified heater model

Instead of solving the temperature field in the heater, a simplified integral model is used for the calculation of the heater temperature, T_H.

Let P_{rad} be net heater radiation power toward the crucible and P_{loss}—power of all the other heat losses in heater, see Fig. 1. P_{rad} is calculated during coupled temperature-radiation problem (Section 2.5). For a chosen basic state for the heater (indicated by index "0") we assume that heater temperature is constant, therefore

$$P_{H,0} - P_{rad,0} - P_{loss,0} = 0. \tag{2}$$

Changes of heater temperature in a non-stationary case are described by the equation

$$P_H - P_{rad} - P_{loss} = C_{p,H}\frac{dT_H}{dt}, \tag{3}$$

where $C_{p,H}$ is heat capacity of the heater.

Assuming that heat losses linearly depend on heater temperature, the following equations hold:

$$P_{loss} = \alpha_{loss}(T_H - T_A), \tag{4}$$

$$P_{loss} - P_{loss,0} = \alpha_{loss}(T_H - T_{H,0}), \tag{5}$$

where T_A is the ambient temperature. The coefficient of proportionality, α_{loss}, depends on the thermal insulation used in the concrete CZ puller.

Combining Eqs. (2), (3) and (5), one obtains

$$C_{p,H}\frac{dT_H}{dt} = \Delta P_H - (P_{rad} - P_{rad,0}) - \alpha_{loss}(T_H - T_{H,0}), \tag{6}$$

where $\Delta P_H = P_H - P_{H,0}$ is the required heater power change computed by PID process control.

The value of α_{loss} can be estimated from heater thermal insulation analysis; in practice, P_{loss} should be small compared to P_H. Using Eqs. (2) and (4) for basic state, one can choose a reasonable value of the ratio $\beta_0 = P_{loss,0}/P_{H,0}$ and obtain an approximation for α_{loss}:

$$\alpha_{loss} = \frac{\beta_0}{1-\beta_0}\frac{P_{rad,0}}{T_{H,0} - T_A}. \tag{7}$$

2.3. Crystallization interface and crystal shape

For the calculation of the time-dependent crystallization interface and crystal shape we use basically the same approach as in Refs. [19,20]. Each time step, Δt, the crystallization interface is moved in normal direction (normal vector $\vec{n}$ is shown in Fig. 1) by the distance $v_n\Delta t$. Front normal velocity in the laboratory reference frame, v_n, is calculated from local heat balance condition after temperature-radiation problem has been solved and heat flux densities at the crystallization interface in crystal and melt (q_c and q_m; $q = \lambda\partial T/\partial n$) have been obtained:

$$v_n = \frac{q_c - q_m}{\rho_c Q} - \vec{V}_p \cdot \vec{n}, \tag{8}$$

where Q is the latent heat of fusion, ρ_c—crystal density, V_p—crystal pulling velocity.

Crystal radius change depends on meniscus angle and crystal growth rate at the TP. After the new shape of the crystallization interface has been obtained, it is shifted downwards by $V_p\Delta t$. The new position of the TP is calculated as the intersection of the crystallization interface tangent and the line which forms an angle of $\phi_{TP} - \phi_0$ with vertical direction at the TP (see Fig. 2), where ϕ_0 is the so-called growth angle. Crystal grows with a constant diameter if the angle ϕ_{TP} between tangent to the free surface at the TP and vertical is equal to ϕ_0.

In the end, the whole crystal (including crystallization interface) is shifted upwards by the distance $V_p\Delta t$.

2.4. Free surface shape

In hydrostatic approximation, the free melt surface shape in the CZ process is determined by hydrostatic pressure and surface tension. In general, both principal curvatures of the free surface have to be taken into account, especially for the seeding stage, when crystal radius is small.

The numerically computed solutions of the Young–Laplace equation (in parametric form, see, e.g., [11, chap. 8]) considering both curvature radii are used in our calculation program. In Fig. 3, the influence of the second curvature radius is illustrated for silicon growth for different values of r_0, the radial coordinate of the uppermost meniscus point. These shapes are shifted along the horizontal axis and compared to the planar analytic solution, which corresponds to very large (infinite) crystal radius. Since signs of the meridional curvature radius, R_1, and second curvature radius, R_2, are opposite and tension forces due to second curvature act in the direction of the symmetry axis, R_1 is smaller for cases with larger second curvature, R_2^{-1}, i.e., for smaller r_0. As a consequence, the maximal meniscus height is also smaller in this case.

It can be seen that, for $r_0 > 50$ mm, free surface shape does not depend significantly on r_0, therefore, to improve calculation speed for larger crystals, optionally, the second curvature radius can be neglected in our calculation program. Under this assumption, free surface shape $y(x)$ in the local coordinate system (x, y), see Fig. 2, is

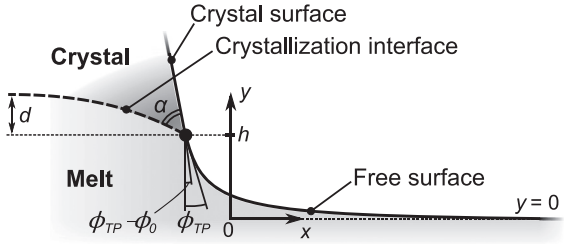

Fig. 2. Schematics of free surface and crystal shape calculation.

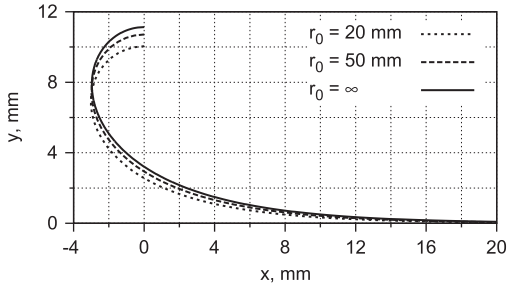

Fig. 3. The influence of second curvature radius on the free surface shape. For comparison purposes, profiles are shifted in horizontal direction (coordinate x is not radius). Silicon physical properties (see Table 1) are considered.

described by the Young–Laplace equation

$$\gamma\frac{1}{R_1}=\gamma\frac{y''}{(1+y'^2)^{3/2}}=\rho g y, \tag{9}$$

which has analytical solution (see, e.g., Ref. [21])

$$x=l_c\,\mathrm{arccosh}\,\frac{2l_c}{y}-l_c\sqrt{4-\frac{y^2}{l_c^2}}+x_0, \tag{10}$$

where γ is the surface tension, ρ – fluid density, $g=9.81$ m/s^2 – gravity, $l_c=\sqrt{\gamma/(\rho g)}$ – capillary constant. From Eq. (10) follows the relation between meniscus height, h, and free surface angle ϕ_{TP} with vertical at TP: $h=l_c\sqrt{2(1-\sin\phi_{TP})}$. x_0 is found from the condition that $y=h$ at $x=0$.

The expression (10) is applied for large values of y: free surface is constructed using the curve $x(y)$. For small y, the curve $y(x)$ is used instead. It is straightforward to show that the following approximation holds in this case:

$$y\approx 4l_c\exp\left(2-\frac{x-x_0}{l_c}\right). \tag{11}$$

Both the precise solution (10) and approximate solution for small y (11) are plotted in Fig. 4. The latter can be safely used for $y<0.2l_c$.

2.5. Temperature in crystal and melt and radiation

Non-stationary axisymmetric temperature fields, $T(r,z,t)$, in crystal and melt domains are obtained by solving the corresponding temperature equation in each of these domains separately:

$$\rho c_p\frac{\partial T}{\partial t}=\frac{1}{r}\frac{\partial}{\partial r}\left[r\lambda\frac{\partial T}{\partial r}\right]+\frac{\partial}{\partial z}\left[\lambda\frac{\partial T}{\partial z}\right], \tag{12}$$

where ρ is density, c_p – specific heat capacity, $\lambda=\lambda(T)$ – thermal conductivity. The corresponding material properties of crystal and melt from Table 1 are used.

For the temperature field the following boundary conditions are applied: temperature is set to melting point at the crystallization interface; $\partial T/\partial r=0$ at the symmetry axis ($r=0$); $\lambda(T)\partial T/\partial n=-q_{rad}$ at all radiating surfaces (normal is outer-pointing). q_{rad} is net radiation heat flux density, obtained from thermal radiation calculations.

Radiation calculation is done in the same way as in Ref. [22], i.e., following Ref. [23]: only diffuse radiation is considered, surfaces are assumed to be opaque and optically gray. Since we do not consider the whole CZ system, including water-cooled vessel wall, the concept of "space node" [22] is still used to include the effect of surroundings.

For each time step thermal radiation and temperature calculations are done iteratively until temperature changes reach the specified convergence criterion.

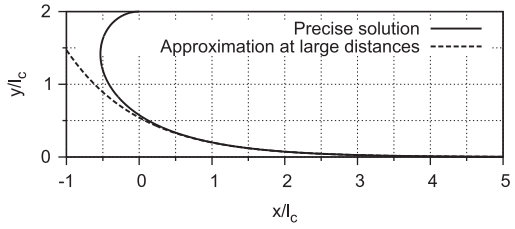

Fig. 4. Precise solution and approximation of the free surface shape neglecting second curvature radius.

Table 1
Material properties of silicon and graphite used in the present work as well as quasi-stationary (QS) growth parameters for the modeled system [22,16,27].

Property	Denotation and value
Melting point	$T_0=1685$ K
Density, melt	$\rho_m=2580$ kg/m^3
Density, crystal	$\rho_c=2329$ kg/m^3
Specific heat capacity, melt	$c_{p,m}=960$ J/(kg K)
Specific heat capacity, crystal	$c_{p,c}=1032$ J/(kg K)
Thermal conductivity, crystal	$\lambda_c(T_0)=22$ W/(m K)
Latent heat of fusion	$Q=1.8\times10^6$ J/kg
Surface tension	$\gamma=0.7835$ N/m
Growth angle	$\phi_0=11^\circ$
Emissivity, melt	$\varepsilon_m=0.30$
Emissivity, crystal	$\varepsilon_c(T_0)=0.46$
Emissivity, graphite	$\varepsilon_{gr}=0.80$
Ambient temperature	$T_A=380$ K
Effective thermal conductivity, melt	$\lambda_{m,eff}=140$ W/(m K)
QS temperature	$T_{H,0}=2167.7$ K
QS radiation power	$P_{rad,0}=204.08$ kW
Heat loss coefficient	$\alpha_{loss}=55.58$ W/K
Heater heat capacity	$C_{p,H}=456.2$ kJ/K
Target pulling velocity	$V_{p,0}=1.0$ mm/min

3. Calculation example of start cone growth

To analyze highly transient processes in CZ system and their impact on the TP region, the growth of the crystal start cone with PID control is calculated with program CZ-Trans. An example of linear transition of crystal radius from 20 mm to 100 mm over crystal length of ca. 107 mm is considered (R_0 in Fig. 5b). As the target pulling velocity 1.0 mm/min is considered for the whole cone growth and for the cylindrical growth afterwards.

Material properties of silicon are readily available in the literature, see, e.g., Refs. [24–26]. The experimentally obtained values can slightly differ because of the differences in experimental methods and system conditions. To be consistent with our previous calculations, we mainly use the same set of physical parameters, following the latest measurements but not adopting them immediately. In the present paper a combination of parameters from Refs. [16,22] is used, as well as value of surface tension reported in Ref. [27]. A summary of all calculation parameters is given in Table 1. Emissivity of graphite is considered for heater and crucible surfaces; for solid silicon the following temperature dependencies of emissivity and thermal conductivity are used [22]:

$$\frac{\varepsilon_c(T)}{\varepsilon_c(T_0)}=\begin{cases}1.39, & T<0.593T_0\\ 1.96-0.96T/T_0, & T\geq 0.593T_0\end{cases},$$

$$\frac{\lambda_c(T)}{\lambda_c(T_0)}=4.495-7.222\frac{T}{T_0}+3.728\left(\frac{T}{T_0}\right)^2.$$

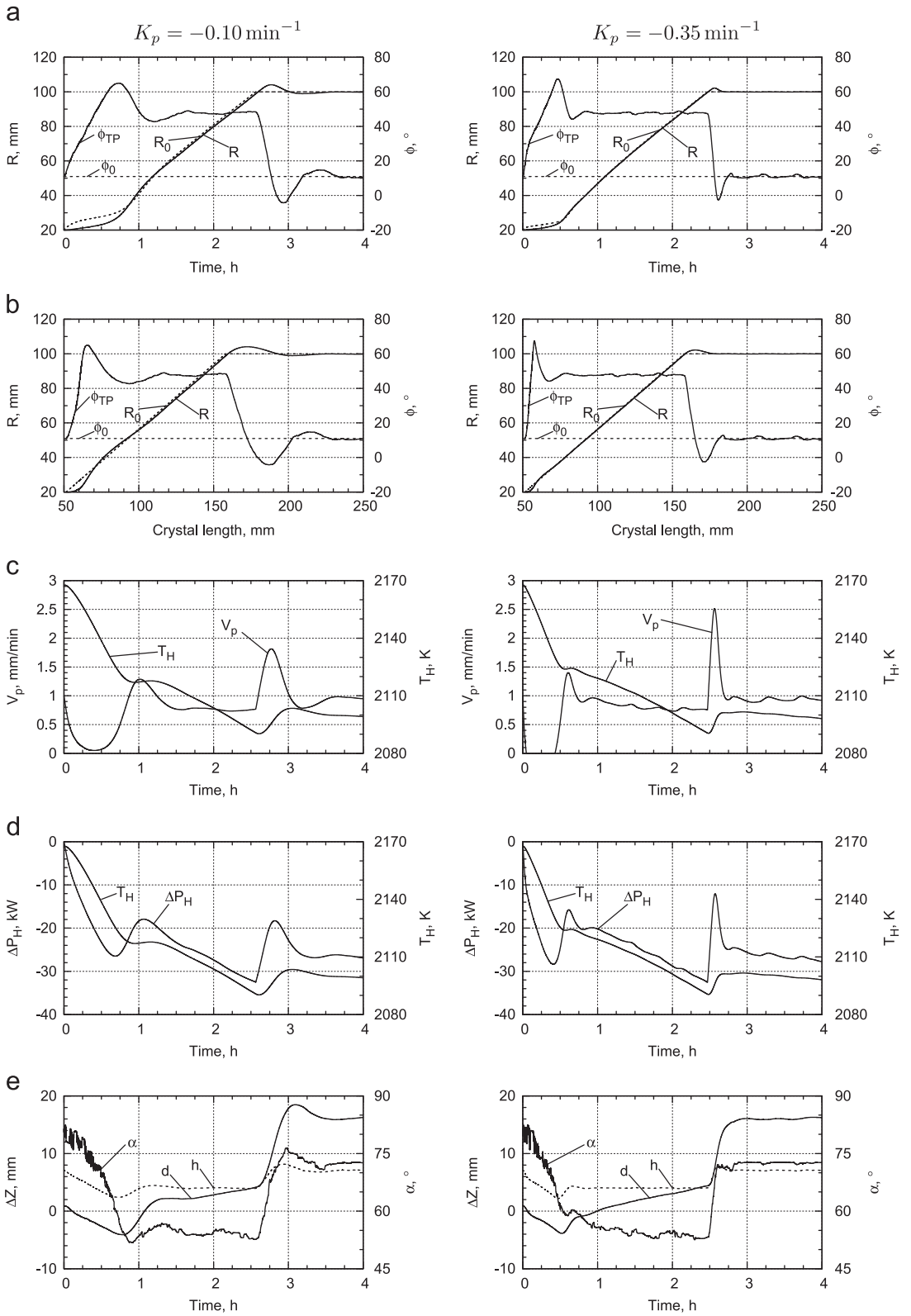

Fig. 5. Calculation results for $K_p^D = -0.10\,\mathrm{min}^{-1}$ (left) and $-0.35\,\mathrm{min}^{-1}$ (right). Time dependencies of (a) crystal radius, R, and meniscus angle at TP, ϕ_{TP}; (b) the same quantities as functions of crystal length; (c) pulling velocity, V_p, and heater temperature, T_H; (d) heater temperature, T_H, and heater power change, ΔP_H; (e) angle α between crystallization interface and crystal side surface at TP, crystallization interface depth, d, and TP height h above melt level.

For a crystal diameter PID controller two different values of parameter K_p^D were used: $-0.10\,\mathrm{min}^{-1}$ and $-0.35\,\mathrm{min}^{-1}$ (it was increased to reduce crystal radius overshoot); integral and derivative terms were switched off. For a heater power PID controller K_p^H was −10 kW min/mm and T_i^H was 1000 s; derivative term was switched off. These values mainly are the result of several numerical test calculations but orders of magnitude are also based on our practical experience of industrial CZ Si growth. We would also like to note that the derivative term of crystal diameter controller was switched off to reduce pulling velocity fluctuations.

Test calculations with various finite element numbers and time steps have been carried out during the development and testing of the program CZ-Trans. The corresponding results allow us to consider the presented calculation example of start cone growth as sufficiently precise.

First, using CZ-Trans, the quasi-stationary state is obtained for a relatively small cylindrical crystal with radius 20 mm and length 50 mm. This state is used as basic state for the further calculations. The heater temperature value, $T_{H,0}$, and net radiation power, $P_{rad,0}$, are found which ensure the TP height which corresponds to cylindrical growth with the considered crystal radius and $V_p = 1.0$ mm/min at the given ambient temperature value T_A. By requiring that heat losses in basic state, $P_{loss,0}$, are ca. 32% of $P_{H,0}$ and using Eq. (7), value of $\alpha_{loss} = 55.58$ W/K is obtained. $C_{p,H}$ is estimated by using specific heat capacity of graphite of 1800 J/(kg K) and mass of graphite parts of ca. 250 kg.

Then the fully transient calculation with CZ-Trans is started at time instant $t=0$ h. Crystal pulling velocity and heater power are adjusted by PID control to obtain increasing radius according to predefined target radius function over the crystal length. Cylindrical growth is continued when target radius of 100 mm is reached.

Calculated time dependencies of crystal radius, R, and meniscus angle at TP, ϕ_{TP}, as well as target crystal radius, R_0, for the considered cone growth are shown in Fig. 5a. The same dependencies as functions of crystal length are given in Fig. 5b. Corresponding time dependencies for the pulling velocity, V_p, heater power change, ΔP_H, and heater temperature, T_H, are shown Fig. 5c,d. Fig. 5e shows the time dependencies for angle α between crystallization interface and crystal side surface at TP, crystallization interface depth (deflection), d, and TP height h above melt level (see also Fig. 2).

Fig. 6 demonstrates the unstructured finite element mesh and temperature field in crystal and melt for three subsequent time instants of the calculation: starting geometry; intermediate state during cone growth; transition from cone to cylinder (i.e., shouldering). Cylindrical growth with radius of 100 mm is illustrated in Fig. 7. It can be seen that the used automatic meshing generates the finite elements progressively larger in regions which are further from the crystallization interface to save the necessary computing resources. Nevertheless, the calculated shape of the crystal side surface is stored as a line with the resolution obtained during the calculation of the new TP position after each time step, see Fig. 7. The nodes of the elements for temperature and radiation calculation are slided along this line during mesh generation. Fig. 8 shows the calculated shape of the interfaces and used finite element mesh in the vicinity of TP during shouldering and cylindrical growth.

4. Analysis of the transient behavior of the CZ system during crystal cone growth

For the analysis of the transient behavior of the PID controlled CZ system during crystal cone growth, the calculated time dependencies in Fig. 5 are used. First, the results for crystal diameter controller gain $K_p^D = -0.10$ min^{-1} are discussed; then the effect of increasing K_p^D to −0.35 min^{-1} is explained.

4.1. Crystal diameter controller gain $K_p^D = -0.10$ min^{-1}

The modeling of the cone growth process is started with cylindrical growth of relatively small crystal with radius 20 mm and $\phi_{TP} = \phi_0$. Because the target radius function demands at $t=0$ h a linear increase of radius over the length of the crystal and initial heater temperature is too high to ensure the required ϕ_{TP}, the PID control significantly reduces the pulling velocity from target value of 1.0 mm/min to ca. 0.1 mm/min in less than 30 min. Correspondingly, h reduces from 7 mm to 2 mm, which causes the increase of ϕ_{TP} from 11° to about 65°. Due to reduced pulling velocity, the PID control reduces the heater power. However, the thermal inertia of heater demands about 1 h to reduce the heater temperature

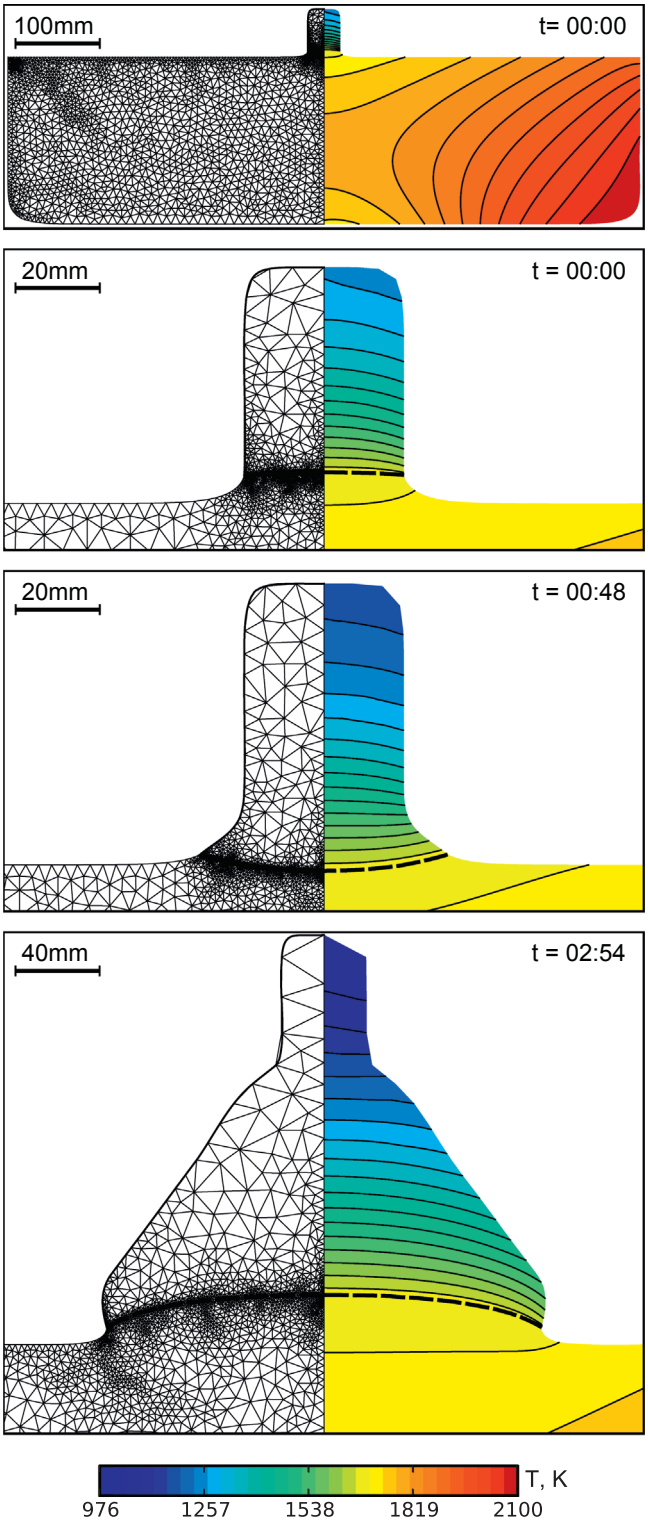

Fig. 6. Finite element mesh and temperature distribution within the melt and crystal during cone growth for $K_p^D = -0.10$ min^{-1}. Shown is also the crystallization interface shape (dashed line).

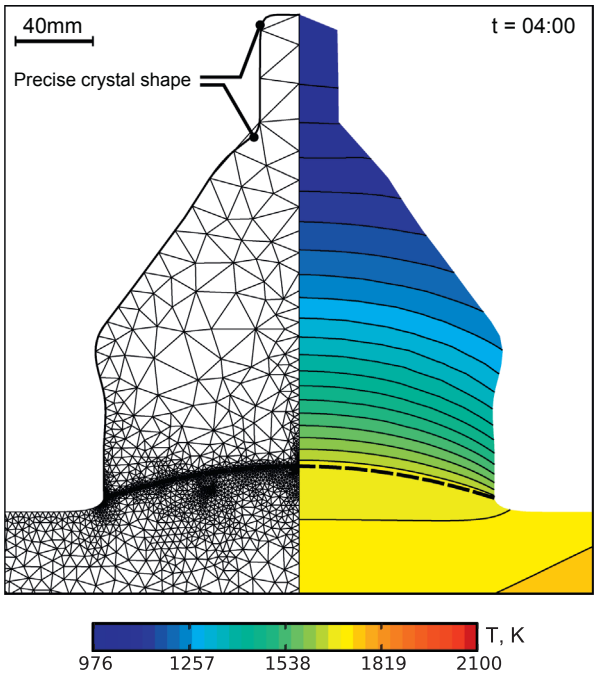

Fig. 7. Finite element mesh and temperature distribution within the melt and crystal during cylindrical growth for $K_p^D = -0.10\ \mathrm{min}^{-1}$. Shown is also the crystallization interface shape (dashed line).

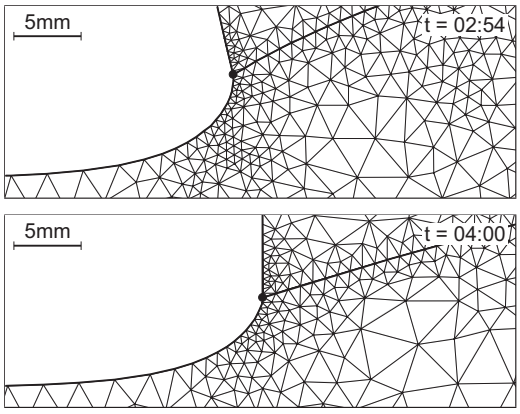

Fig. 8. Shape of phase boundaries and finite element mesh in the TP region for $K_p^D = -0.10\ \mathrm{min}^{-1}$.

sufficiently to obtain pulling velocity of ca. 0.8 mm/min, which is slightly smaller than target value.

After approximately 1 h process time, crystal pulling velocity and heater power overshoots are observed, which are caused by a sophisticated interplay between the CZ system and the corresponding process controls. Due to high initial heater temperature, it is gradually decreased, cooling the melt and increasing crystal growth velocity, but, apparently, the initial (for $t = 0\ldots0.5$ h) rate of cooling is considerably higher than the rate required during cone growth when V_p is approximately constant (for $t = 1.5\ldots2.5$ h). Once T_H has been decreased sufficiently, the overshoot of pulling velocity prevents too rapid increase of crystal radius and causes the change of heater power to compensate the change of V_p.

After the mentioned transition time of about 1 h, i.e., starting from $t = 1.5$ h, the cone is grown with the almost target pulling velocity for the whole cone. The meniscus angle is about 47°. However, at larger crystal radius values, the TP comes closer to hot melt region near crucible wall, therefore the heater power must be gradually reduced to gradually reduce its temperature. It can be seen that the PID control ensures this reduction well.

After 2.5 h process time, the transition from cone to cylindrical growth is started. This demands the decrease of meniscus angle to $\phi_\mathrm{TP} = \phi_0$, i.e., increase of TP height; therefore the PID control enhances the pulling velocity. Since the desired crystal shape is not smooth, pulling velocity has to be increased considerably, and, because only proportional part is used for the control, crystal radius overshoot occurs. Simultaneously, the crystal shape bulge ensures higher radiation heat losses which increases the growth velocity, therefore the TP height needs some overshoot of pulling velocity (for about 30 min) to compensate this. The increase of pulling velocity causes the sharp increase of heater power and with some time delay the increase of heater temperature, which is smooth due to thermal inertia of heater. During transition to cylindrical growth oscillations of ϕ_TP occur; ϕ_TP even becomes negative (see also Figs. 6 and 8 at $t = 2$ h 45 min), however, process control successfully handles the situation and makes them to vanish.

Fig. 5e shows that the angle α during cone growth is about 55° and, because the slope of the cone is about 53°, the crystallization interface at TP forms an angle of 92° with vertical. During cylindrical growth the crystallization interface angle is about 73°. It can be seen that the crystallization interface at the beginning of the cone is even convex (see Fig. 6, $t = 48$ min); in the cone region after 1 h it becomes concave but is relatively flat (deflection smaller than 5 mm); after the transition to the cylindrical growth the crystallization interface becomes concave and the deflection increases about three times, i.e., to ca. 15 mm.

4.2. Crystal diameter controller gain $K_p^D = -0.35\ \mathrm{min}^{-1}$

The qualitative tendencies for case with $K_p^D = -0.35\ \mathrm{min}^{-1}$ are practically the same as for $K_p^D = -0.10\ \mathrm{min}^{-1}$: first, crystal pulling velocity and heater power are decreased to ensure the increase of crystal diameter; when the transition to cylindrical growth begins, crystal pulling velocity is considerably increased for a short time interval, which leads to the increase of heater power and its temperature. Similarly as before, during almost the whole first hour of simulation, crystallization interface is convex but it changes to concave at later times.

Due to the increased $K_p{}^D$, pulling velocity is adjusted more rapidly; it is, in fact, dropped to zero in the first 30 min, indicating that the heater temperature has to be dropped first, and only after that the crystal pulling can be started. Increased $K_p{}^D$ also produces a more rapid oscillations of V_p, which may be undesirable.

The most visible difference compared to previously considered $K_p{}^D$ is that now crystal radius more closely follows the desired shape, and the overshoot due to transition to cylindrical growth is a few times smaller. Of course, in a real world more careful considerations should be taken into account for the design and parameters of the process control.

5. Conclusions

The proposed mathematical model of transient CZ process, calculation algorithm and implementation in calculation program CZ-Trans can accurately describe the vicinity of the triple point and can distinguish very small crystal shape changes and therefore can be effectively used for the modeling of CZ process with optical crystal diameter control by changing crystal pulling velocity and heater power. For a considered calculation example, crystal–melt interface is convex at initial stage of the cone growth and then changes to concave. Overshoot of crystal radius at the transition to cylindrical growth was observed due to imposed non-smooth

desired crystal shape, and was reduced by adjusting control parameters. The optimal design and tuning of CZ control is a difficult topic which is beyond the scope of this paper. However, CZ-Trans can be used for testing of the effectiveness of different CZ control designs.

Acknowledgment

The present work is carried out at the University of Latvia and has been supported by the European Regional Development Fund, project contract No. 2011/0002/2DP/2.1.1.1.0/10/APIA/VIAA/085.

References

[1] D. Lukanin, V. Kalaev, Y. Makarov, T. Wetzel, J. Virbulis, W. von Ammon, Advances in the simulation of heat transfer and prediction of the melt-crystal interface shape in silicon CZ growth, Journal of Crystal Growth 266 (2004) 20–27, Proceedings of the Fourth International Workshop on Modeling in Crystal Growth.
[2] N.V. den Bogaert, F. Dupret, Dynamic global simulation of the Czochralski process I. Principles of the method, Journal of Crystal Growth 171 (1997) 65–76.
[3] N.V. den Bogaert, F. Dupret, Dynamic global simulation of the Czochralski process II. Analysis of the growth of a germanium crystal, Journal of Crystal Growth 171 (1997) 77–93.
[4] V. Mamedov, M. Vasiliev, V. Yuferev, D. Pantsurkin, V. Shlegel, Y. Vasiliev, Control of multi-zone resistive heater in low temperature gradient BGO Czochralski growth with a weighing feedback, based on the global dynamic heat transfer model, Journal of Crystal Growth 312 (2010) 2814–2822.
[5] V. Mamedov, M. Vasiliev, V. Yuferev, Dynamic global model of oxide Czochralski process with weighing control, Journal of Crystal Growth 318 (2011) 703–707, The 16th International Conference on Crystal Growth (ICCG16)/The 14th International Conference on Vapor Growth and Epitaxy (ICVGE14).
[6] N. Duanmu, Modeling, Dynamics, and Control of the Czochralski Crystal Growth Process, Ph.D. Thesis, College of Engineering, Boston University, 2006.
[7] M. Gevelber, D. Wilson, N. Duanmu, Modelling requirements for development of an advanced Czochralski control system, Journal of Crystal Growth 230 (2001) 217–223 Proceedings of the Third International Workshop on Modeling in Crystal Growth.
[8] J. Winkler, M. Neubert, J. Rudolph, Nonlinear model-based control of the Czochralski process I: motivation, modeling and feedback controller design, Journal of Crystal Growth 312 (2010) 1005–1018.
[9] J. Winkler, M. Neubert, J. Rudolph, Nonlinear model-based control of the Czochralski process II: reconstruction of crystal radius and growth rate from the weighing signal, Journal of Crystal Growth 312 (2010) 1019–1028.
[10] M. Neubert, J. Winkler, Nonlinear model-based control of the Czochralski process III: proper choice of manipulated variables and controller parameter scheduling, Journal of Crystal Growth 360 (2012) 3–11 5th International Workshop on Crystal Growth Technology.
[11] T. Duffar (Ed.), Crystal Growth Processes Based on Capillarity, John Wiley & Sons, Ltd, 2010.
[12] A. Raufeisen, M. Breuer, T. Botsch, A. Delgado, Transient 3D simulation of Czochralski crystal growth considering diameter variations, Journal of Crystal Growth 311 (2009) 695–697, The Proceedings of the 4th International Asian Conference on Crystal Growth and Crystal Technology.
[13] A. Raufeisen, M. Breuer, T. Botsch, A. Delgado, Prediction of the three-phase boundary movement in Czochralski crystal growth, Journal of Crystal Growth 312 (2010) 2297–2299.
[14] O. Weinstein, W. Miller, Three-dimensional calculations of facets during Czochralski crystal growth, Journal of Crystal Growth 312 (2010) 989–996.
[15] The cgsim package, ⟨http://www.str-soft.com/products/CGSim/⟩, December 16, 2012.
[16] V. Kalaev, I. Evstratov, Y. Makarov, Gas flow effect on global heat transport and melt convection in Czochralski silicon growth, Journal of Crystal Growth 249 (2003) 87–99.
[17] The femag-cz software, ⟨http://www.femagsoft.com/products/czochralski-cz-process.html⟩, December 16, 2012.
[18] F. Dupret, R. Rolinsky, L. Wu, F. Loix, A. De Potter, N. Van den Bogaert, V. Regnier, Global simulation of CZ and FZ bulk crystal growth: from quasi-dynamic and dynamic modelling to process control and crystal quality optimization, ECS Transactions 18 (2009) 935–943.
[19] A. Rudevičs, A. Muižnieks, G. Ratnieks, A. Mühlbauer, T. Wetzel, Numerical study of transient behaviour of molten zone during industrial FZ process for large silicon crystal growth, Journal of Crystal Growth 266 (2004) 54–59, Proceedings of the Fourth International Workshop on Modeling in Crystal Growth.
[20] A. Rudevics, A. Muiznieks, H. Riemann, A. Luedge, G. Ratnieks, W. von Ammon, Numerical study and comparisons with experimental data for transient behaviour of phase boundaries during industrial FZ process for silicon crystal growth, Journal of Crystal Growth 275 (2005) e561–e565, Proceedings of the 14th International Conference on Crystal Growth and the 12th International Conference on Vapor Growth and Epitaxy.
[21] G. Batchelor, An Introduction to Fluid Dynamics, Cambridge University Press, 2000.
[22] G. Ratnieks, A. Muižnieks, A. Mühlbauer, Modelling of phase boundaries for large industrial FZ silicon crystal growth with the needle-eye technique, Journal of Crystal Growth 255 (2003) 227–240.
[23] F. Dupret, P. Nicodeme, Y. Ryckmans, P. Wouters, M. Crochet, Global modelling of heat transfer in crystal growth furnaces, International Journal of Heat and Mass Transfer 33 (1990) 1849–1871.
[24] Z. Zhou, S. Mukherjee, W.-K. Rhim, Measurement of thermophysical properties of molten silicon using an upgraded electrostatic levitator, Journal of Crystal Growth 257 (2003) 350–358.
[25] Y. Magomedov, G. Gadjiev, High-temperature thermal conductivity of silicon in the solid and liquid states, High Temperature 46 (2008) 422–424.
[26] R. Hull (Ed.), Properties of Crystalline Silicon, EMIS Datareviews Series, INSPEC, The Institution of Electrical Engineers, 1999.
[27] M. Przyborowski, T. Hibiya, M. Eguchi, I. Egry, Surface tension measurement of molten silicon by the oscillating drop method using electromagnetic levitation, Journal of Crystal Growth 151 (1995) 60–65.